ORIGINAL RESEARCH ARTICLE

Soft Tissue Engineering with Micronized-Gingival Connective Tissues†

Sawako Noda[1], Yoshinori Sumita[1,2*], Seigo Ohba[1], Hideyuki Yamamoto[1], Izumi Asahina[1]

[1]Department of Regenerative Oral Surgery, Nagasaki University Graduate School of Biomedical Sciences, Nagasaki, Japan, [2]Basic and Translational Research Center for Hard Tissue Disease, Nagasaki University Graduate School of Biomedical Sciences, Nagasaki, Japan

Running title: Micronized-gingival connective tissues promote the skin wound healing

Key words: cell-based therapy, micronized-tissues, gingiva, wound healing

*Address correspondence to Associate Professor. Yoshinori Sumita, Basic and Translational Research Center for Hard Tissue Disease, Nagasaki University Graduate School of Biomedical Sciences, 1-7-1 Sakamoto, Nagasaki 852-8588, Japan. Tel: +81 95 819 7706; Fax: +81 95 819 7718; E-mail: y-sumita@nagasaki-u.ac.jp

†This article has been accepted for publication and undergone full peer review but has not been through the copyediting, typesetting, pagination and proofreading process, which may lead to differences between this version and the Version of Record. Please cite this article as doi: [10.1002/jcp.25871]

Additional Supporting Information may be found in the online version of this article.

Received 4 October 2016; Revised 21 February 2017; Accepted 22 February 2017

Journal of Cellular Physiology

DOI 10.1002/jcp.25871

Abstract

The free gingival graft (FGG) and connective tissue graft (CTG) are currently considered to be the gold standards for keratinized gingival tissue reconstruction and augmentation. However, these procedures have some disadvantages in harvesting large grafts, such as donor-site morbidity as well as insufficient gingival width and thickness at the recipient site post-treatment. To solve these problems, we focused on an alternative strategy using micronized tissue transplantation (micro-graft). In this study, we first investigated whether transplantation of micronized gingival connective tissues (MGCTs) promotes skin wound healing. MGCTs (≤100 μm) were obtained by mincing a small piece (8 mm^3) of porcine keratinized gingiva using the RIGENERA system. The MGCTs were then transplanted to a full skin defect (5 mm in diameter) on the dorsal surface of immunodeficient mice after seeding to an atelocollagen matrix. Transplantations of atelocollagen matrixes with and without micronized dermis were employed as experimental controls. The results indicated that MGCTs markedly promote the vascularization and epithelialization of the defect area 14 days after transplantation compared to the experimental controls. After 21 days, complete wound closure with low contraction was obtained only in the MGCT grafts. Tracking analysis of transplanted MGCTs revealed that some mesenchymal cells derived from MGCTs can survive during healing and may function to assist in wound healing. We propose here that micro-grafting with MGCTs represents an alternative strategy for keratinized tissue reconstruction that is characterized by low morbidity and ready availability.

Introduction

In dental implant therapy, it is crucial to obtain an adequate volume (width and thickness) of keratinized gingiva to maintain healthy peri-implant tissues, since an insufficient volume results in unsatisfactory esthetic outcomes as well as gingival inflammation due to poor plaque control (Thoma et al., 2009; Herford et al., 2010; Schmitt et al., 2013). Meanwhile, alveolar bone atrophy after tooth extraction leads to a simultaneous decline in keratinized gingiva. Therefore, the reconstruction or augmentation of keratinized mucosa after bone augmentation and/or dental-implant placement is necessary to ensure the survival of the dental implant and to improve the aesthetic qualities (Kim et al., 2009; Schrott et al., 2009; Lin et al., 2013; Brito et al., 2014; Schmitt et al., 2015). Currently, the free gingival graft (FGG) and connective tissue graft (CTG) are considered to be the gold standards for keratinized tissue augmentation (Thoma et al., 2009; Herford et al., 2010; Agarwal et al., 2015). However, these procedures have some disadvantages in the harvest of large grafts, such as donor-site morbidity and insufficient gingival width and thickness at the recipient site (Thoma et al., 2009; Herford et al., 2010; Schmitt et al., 2014; Schmitt et al., 2015). Therefore, an alternative strategy that avoids donor-site morbidity but has comparable healing potential is needed.

Recently, soft tissue engineering using biomaterials and/or stem cells has been an area of increasing focus (Imaizumi et al., 2004; Wu et al., 2007; Basiouny et al., 2011). For example, as an alternative to autogenous tissues, material of allo- or xeno-genic origin, such as acellular human dermal matrix (ADM) and porcine collagen matrix (CM), have been investigated in clinical trials as methods for

increasing the volume of keratinized tissues (Herford et al., 2010; Schmitt et al., 2013; Schmitt et al., 2015; Agarwal et al., 2015; Basegmez et al., 2013). However, although ADM or CM showed utility in augmenting the keratinized mucosa without donor-site morbidity, the peri-implant keratinized gingiva regenerated using these materials could not provide sufficient width and thickness without shrinkage compared to FGG (Agarwal et al., 2015). Meanwhile, it has been shown that gingival mucosa-derived mesenchymal stem cells (GMMSCs) are able to promote wound healing (Zhang et al., 2010; Zhang et al., 2012; Fournier et al., 2013; Boink et al., 2015). Compared to dermal MSCs, GMMSCs showed greater proliferation and migration capacity without influencing matrix contraction or α-smooth muscle actin (α-SMA) expression in skin wounds. (Boink et al., 2015) In fact, several studies have demonstrated that GMMSCs are associated with superior scar quality while dermal MSCs or subcutaneous adipose MSCs are associated with normotrophic- or hypertrophic-scar formation (Boink et al., 2015; van den Broek et al., 2014; van den Bogaerdt et al., 2013). Therefore, gingival tissue can be considered to be an excellent stem cell source for soft tissue engineering. However, in the clinical use of GMMSCs, obtaining sufficient numbers of GMMSCs may be challenging because an expansion process is required *in vitro*. In fact, the plasticity of MSCs declines sharply during culture expansion and cell passaging (Agata et al., 2010; Xia et al., 2013). .

On the other hand, new possibilities for minimally invasive and non-laborious procedures using fresh non-cultured cells obtained from small amounts of autologous tissues, such as bone marrow, adipose, and dermal tissues, have been suggested from recent research on cell-based therapies in tissue

engineering (Sumita et al., 2011; I et al., 2014; Yoo et al., 2009). For example, it was recently reported that the transplantation of micronized tissues (micro-graft) 50 μm in size from small autologous tissue samples (only a few millimeters in size) can be used effectively for bone or soft tissue engineering (Giaccone et al., 2014; Zanzottera et al., 2014; Trovato et al., 2015; Monti et al.,2016; Marcarelli et al., 2016; Svolacchia et al., 2016). In particular, micro-grafts from adipose or dermal connective tissues have been shown to improve wound healing or hair-growth (Giaccone et al., 2014; Zanzottera et al., 2014; Marcarelli et al., 2016; Svolacchia et al., 2016). With respect to the micro-graft, stem/progenitor cells, as well as extracellular matrix (ECM) components and growth factors, are thought to enrich the micronized tissue suspension (Svolacchia et al., 2016). Moreover, this procedure can be carried out easily and safely by using a dedicated device, such as Rigenera® system, during the intervention in the operating room. Therefore, the micro-graft continues to evolve as a concept and can be further developed as an alternative strategy for facilitating the use of cell-based therapies in the clinical setting.

This study aims to develop a new strategy of applying micro-grafts of gingival connective tissue for reconstructing or augmenting the keratinized mucosa as an alternative to FGG or CTG. We first investigated whether transplantation of micronized gingival connective tissues (MGCTs) promotes skin wound healing. MGCTs were obtained from small (approximately 8-mm^3) keratinized gingival connective tissue samples, and contain GMMSCs, which are known to promote wound healing with superior scar quality (Boink et al., 2015). Therefore, micro-grafts of gingival connective tissue have the potential to

contribute to soft tissue engineering by their low morbidity and ready availability.

Materials and Methods

Micronization of gingival connective tissues

All procedures with animals were carried out under the protocol approved by the Facility Animal Care Committee of Nagasaki University (1310111096-2). A piece (2 cubic millimeter of size) of keratinized-gingival connective tissue was harvested from the palatal mucosa of freshly slaughtered 6-month-old pig (Fig. 1A). Then, a harvested tissue was mechanically dissociated right away with Rigenera® system using Rigenera® machine and Rigeneracons®, a mechanical disruptor of small tissues (Human Brain Wave, Italy), according to a method previously described (Zanzottera et al., 2014; Trovato et al., 2015; Marcarelli et al., 2016) (Fig. 1B). Briefly, a harvested tissue was inserted in the Rigeneracons (which are composed of a grid provided by hexagonal blades) with the addition of 1 ml of saline solution per piece, and micronized for 90 second by Rigenera machine (Fig. 1B). Then, after centrifuge, the precipitated micronized-gingival connective tissues (MGCTs, ≤100 μm each) was suspended in 200 μl of Dulbecco's Modified Eagle's Medium (DMEM; Sigma, St. Louis, MO, USA) [For reference, a considerable number of MGCTs adhered to the culture dish and expressed a mesenchymal cell marker (anti-Vimentin antibody) when seeded into a 10 cm culture dish and cultured in DMEM containing 10 % fetal bovine-serum and 2 % antibiotic-antimycotic solution for 7 days (Fig. 1C)], and subsequently, MGCTs were re-suspended and seeded onto an atelocollagen-matrix, which size was approximately 6 mm in diameter and 2 mm in thickness (TERUDERMIS®; Olympus Terumo Biomaterials, Tokyo, Japan), just before the transplantation (Fig. 1D).

In order to track the donor cells post-transplantation, some MGCTs were labeled with PKH26 (red fluorescent cell linker kit; Sigma, St. Louis, MO, USA). In addition, micronized-skin (dermal) connective tissues were employed as one of experimental controls.

Transplantation of micronized-tissues

8-week-old female BALB/cAJcl-nu/nu mice (Nihoncrea, Tokyo, Japan) were anesthetized with an intraperitoneal injection of sodium pentobarbital (15 mg/kg) (Nembutal; Dainippon Sumitomo Pharama, Osaka, Japan). During and after operation, mice were kept warming. A 5 mm (in diameter) round full-thickness excisional wound was made on the back of mice (Fig. 1E). Subsequently, samples were transplanted to the skin-defect and positioned down over the wound bed. Then, to measure the contraction level, 4 tattoo marks were delineated at the place of 1 mm away from the wound margin. Finally, a donut-shaped flexible silicone splint with a 10 mm inner and 16 mm outer diameter was fixed to the skin around the wound with interrupted 5-0 nylon sutures and an adhesive film (Fig. 1F). Experiments were performed in each experimental group, such as only defects without any grafts [Control; n=5 at each time point, total n=15], grafts of atelocollagen-matrix with only DMEM [AC; n=8 at 7 and 14 days post-transplantation, n=5 at 21 days post-transplantation, total n=21], micro-grafts of MGCTs with atelocollagen-matrix [MG; n=8 at 7 and 14 days post-transplantation, n=5 at 21 days post-transplantation, total n=21], and micro-grafts of micronized-dermis with atelocollagen-matrix [MG-Skin; each n=5 at two

time points (7 and 14 days post-transplantation), total n=10]. Furthermore, an additional *in vivo* experiment using PKH26-labeled MGCTs were performed as MG-group [MG and AC (negative control); n=3 at 7 days post-transplantation].

Measurements of wound closure and contraction

After 7, 14, and 21 days of transplantation, digital photographs of wound area on the back of each mouse, which was laid as flat as possible, were taken and then were scanned into a computer. The percentage of wound-closure was calculated, as "area of actual wound / area of original wound", with an image analysis program (Image J; NIH, Bethesda, MD, USA). The percentage of wound-contraction was also calculated as reduction rate by which the area of actual tattoo marks was subtracted from the initial tattooed area. Tattooed area was presented with length x breadth of the length between opposite tattoos.

Histological and immunohistological analysis

At 7, 14, and 21 days post-transplantation, the specimens were harvested and fixed with 4% paraformaldehyde. Then, they are embedded in paraffin wax. Sections (3-μm thickness) were deparaffinized and routinely stained with hematoxylin & eosin (HE) and Masson's trichrome for conventional morphological evaluation. To measure the epithelial thickness on samples of MG- and MG-Skin-groups at 14 days post-transplantation, 10 random sites in hematoxylin and eosin-stained sections (3 sets of

consecutive 3 sections were examined per mouse; 3 specimens/group) under x200 magnification were measured by Lumina vision software (MITANI, Tokyo, Japan). Two examiners independently counted the thickness randomly chosen from the length of 3 consecutive sections composed of both edge directions from central point of wound-area.

To confirm the re-epithelization, immunohistochemical staining was performed with Vectastain ABC kit (Vector, Burlingame, CA, USA). Sections were stained with mouse monoclonal anti-pan Cytokeratin (1:100) (Abcam, Cambridge, UK) antibody. Then, specimens were finally reacted with 0.1 %w/v 3.3'-diaminobenzidine tetrahydrochloride (DAB immunohistochemistry; GenWay, CA, USA) in PBS and counterstained with hematoxylin. Control staining was performed by replacing the first antibody with pre-immune serum eluted from the corresponding affinity columns.

Furthermore, to assess the blood vessel formation, immunofluorescence staining was performed with rabbit polyclonal anti-mouse vWF (1:100) (Blood Vessel Staining Kit; Millipore, Billerica, MA, USA) and rabbit polyclonal anti-mouse CD31 (1:50) (Abcam, Cambridge, UK) antibodies. The slides were then incubated with Alexa-Flour 546-conjugated goat anti-rabbit (1:100) (Invitrogen, Carlsbbad, CA, USA) for vWF and Alexa-Flour 488-conjugated donkey anti-rabbit (1:100) (Invitrogen) for CD31 as secondary-antibodies. Then, 4′,6-diamidino-2-phenylindole, dihydrochloride (DAPI; Invitrogen) was added for 3-5 minutes. Control staining was performed by replacing the first antibody with pre-immune serum eluted from the corresponding affinity columns. The percentage of blood vessel-area (vWF/CD31

stained-area) to whole-area of transplants just under the basement membrane were measured by pixels on Image J software (NIH). This percentage of surface area occupied by blood vessels was assessed under x200 magnification using five randomly fields in a section for 5 sections/specimens (3 specimens/group at each time point).

To detect the donor cells, frozen sample sections (5 μm thickness) from mice after 7 days of transplantation were fixed in 4 % paraformaldehyde, followed by three washing steps in PBS for 5 min each. Then, the sections were observed under a fluorescence microscope to detect PKH26-positive cells in each samples.

Gene expression analysis for detection of MGCT-derived cells and tissue regenerative factors after transplantation

Reverse Transcription Polymerase Chain Reaction (RT-PCR) was used to determine the mRNA expressions of porcine endothelial, mesenchymal or epithelial cell markers to track the MGCT-derived cells in specimens at 14 days post-transplantation. Total RNA was extracted with Trizol-reagent (Invitrogen, CA, USA) from the samples of MG-, AC-, and Control-groups. Total RNA extracted from porcine mucosal tissues was employed as a positive control (Pig-group). First-strand cDNA synthesis was performed by SuperScript First-strand Synthesis (Invitrogen). cDNA was amplified with Takara-Taq (Takara Bio Inc., Shiga, Japan). PCR reactions were performed with Mx3000P QPCR System (Agilent Technologies, CA, USA). Porcine

(*cd31, vWF, vimentin, cytokeratin,* and *β-actin*) and mouse glyceraldehyde-3-phosphate dehydrogenase (*gapdh*) specific primer sets are shown in Table 1.

Quantitative real time-PCR was used to determine the mRNA expressions of tissue regenerative/angiocrine factors (*sdf-1, cxcr-4, vegf-a, -b, flt-1* and *flk-1*) genes in the transplanted specimens at 7 days after transplantation. Total RNA was extracted with Trizol-reagent (Invitrogen), and first-strand complementary DNA synthesis was performed by SuperScript First-Strand Synthesis (Invitrogen). Complementary DNA was amplified with Takara-Taq (Takara Bio). PCR reactions were performed with Mx3000P QPCR System (Agilent Technologies, Santa Clara, CA, USA). Mouse-specific primer sets are shown in Table 2. As internal standards, glyceraldehyde-3-phosphate dehydrogenase (*gapdh*) primer was used for quantitative real time-PCR.

Statistical analysis

Means were analyzed using one-way analysis of variance. Dunnett's multiple comparison t-test was used to detect any significant differences within each group. Experimental values were presented as mean ± s.d. A p-value of < 0.05 was considered to be statistically significant.

Results

Macroscopic findings post-transplantation

At 7 days post-transplantation, re-epithelialization seemed to be under way in all samples and was most advanced in the MG-group (atelocollagen matrix with MGCTs) (Fig. 2A, B). At 14 days, the wound area was obviously reduced in the MG-group (approximately 15% of the original wound area) compared to the other groups (approximately 26% in the AC-group and 40% in the Control-group) (Fig. 2A, B). By 21 days, complete wound closure was observed in the MG-group while wound closure was progressing in the AC- and Control-groups (Fig. 2A, B). Meanwhile, scar contraction was obviously inhibited by treatment with atelocollagen matrix, and MGCTs promoted that effect of the atelocollagen matrix markedly at 14 days post-transplantation (Fig. 2A, C).

Histological observations of the wound area

At day 14 post-transplantation, re-epithelialization progressed obviously along the surface of the atelocollagen-matrix in the MG- and MG-skin groups (Fig. 3A, B, G, H). In contrast, delayed epithelialization was observed in both the AC- and Control-groups (Fig. 3C, D, E, F), while the absorption of atelocollagen-matrix appeared comparable among the transplantation groups with or without micro-grafts (Fig. 3B, D, H). However, numerous inflammatory cells were noted in the matrix area of the AC-group (Fig. 3D). The epithelial thickness of the re-epithelialized area in the MG-group was greater than the

MG-skin-group (Fig. 3I).

At day 21 post-transplantation, the MG-group showed complete epithelialization, and cytokeratin-positive skin appendages were detected only in this group (Fig. 4A). Although re-epithelialization progressed in the AC-group, regeneration of cytokeratin-positive epidermis was incomplete (Fig. 4B). Meanwhile, the Control-group did not show obvious epithelialization, although recovery of the dermis was noted (Fig. 4C).

Blood vessel formation in the wound area

Blood vessels were visualized clearly, using anti-CD31 and -vWF antibodies, in the matrix of the MG-group compared to the AC-group at 14 days post-transplantation (Fig. 5A, B). Further, blood vessel formation was increased in a time-dependent manner (especially at 14 and 21 days) in the MG-group (Fig. 5C).

Detection of MGCT-derived cells and tissue regenerative factors in the wound area

At day 7 post-transplantation, PKH26-labeled (red fluorescent) donor cells were detected mainly in the matrix immediately below the area of epithelialization (Fig. 6A). The expression of porcine-specific mRNAs related to endothelial, mesenchymal, or epithelial cell marker genes were examined in samples at 14 days, and mesenchymal cell signals (*vimentin* gene derived from MGCT-derived cells) were clearly recognized in the MG-group, just as in porcine specimens derived from porcine mucosal tissues (a positive control) (Fig.

6B). However, although the mRNA expression of endothelial and epithelial cells (*cd31*, *vWF* and *cytokeratin* genes) in the MG-group was detected, the expression levels were very low compared with the positive control (Pig-group) (Fig. 6B). Meanwhile, these genes were not expressed in the Control- and AC-groups (Fig. 6B), although the murine *gapdh* gene (housekeeping gene) was expressed in the MG-, AC- and Control-groups (data not shown). While a small number of MGCT-derived cells may have contributed directly to form the blood vessels or epidermis in the wound area, the majority of donor cells likely functioned as mesenchymal cells. Interestingly, at 7 days after transplantation, mouse-specific mRNA expression of SDF-1 that stimulates the vascularization and recruits the MSCs from bone marrow was significantly up-regulated in the MG-group (Fig. 6C). Also, the expression level of CXCR-4 mRNA, which is a receptor of SDF-1 and a crucial factor of cell migration, was higher in the MG-group when compared with the AC-group (Fig. 6C). Consistent with these results, an up-regulation of vasculogenic genes (*vegf-a* and -*b*) and their receptors (*flt-1* and *flk-1*) was seen in the MG-group (Fig 6C).

Discussion

This study demonstrated that tissue engineered micro-grafts of keratinized gingival connective tissue could promote skin regeneration. The positive study outcomes were as follows: 1) MGCTs, obtained from a few millimeters of gingiva, reliably hastened the re-epithelialization of wounds with less scar contraction, 2) MGCTs obviously induced vascularization as explants during the re-epithelialization process, and 3) surviving mesenchymal cells derived from MGCTs might have affected these phenomenon in a paracrine manner. These outcomes indicate that this strategy has potential as an alternative therapy to the conventional FGG or CTG.

In re-epithelialization, approximately 90 % of the wound area was closed at 2 weeks post-transplantation when atelocollagen-matrix was transplanted with MGCTs; in contrast, the same level of wound closure was observed at 3 weeks post-transplantation in the absence of MGCTs. Moreover, the epithelial thickness of the regenerated area was greater in the micro-grafts with MGCTs at 3 weeks compared with the control and atelocollagen alone groups. These findings clarified that MGCTs from small amounts of keratinized gingiva (8 mm^3) can have obvious biological effects on skin regeneration. The Rigenera® system exploits the activities of stem/progenitor cells, ECM components and/or growth factors contained in the micronized tissues. Recently, Graziano A and colleagues proposed a regenerative therapy using the Rigenera® system, and demonstrated that micronized tissues obtained from various human samples, such as periosteum, dental pulp, adipose or dermal tissues, displayed high cell viability and optimal regenerative

potential (Monti et al., 2016; Svolacchia et al., 2016). For example, in wound healing experiments, a 8-mm^3 sample of skin was micronized, yielding approximately 80,000 cells with 92% cell viability. In addition, increased levels of MSC markers, such as CDs34, 90 and 105, were observed in the micronized tissues (Svolacchia et al., 2016). Indeed, micro-graft of skin (dermal) connective tissues has been shown to be effective in improving surgical wound dehiscence or exaggerated scars in clinical trials (Svolacchia et al., 2016). These data suggested that mesenchymal stem/progenitor cells in the micronized connective tissues might play a role in complex wound healing. Meanwhile, recent studies demonstrated that gingival mucosa-derived MSCs (GMMSCs) have greater proliferative and migration capacity compared to skin (dermal) MSCs (Boink et al., 2015). Furthermore, GMMSCs possess not only multipotent differentiation capacity but also immunosuppressive and anti-inflammatory functions (Zhang et al., 2012; Fournier et al., 2013). In fact, it has been shown that GMMSCs promote skin wound healing by eliciting the polarization of macrophages toward an anti-inflammatory M2 phenotype (Zhang et al., 2010). These data may indicate that MGCTs containing such mesenchymal stem/progenitor cells exhibit superior capacity for re-epithelialization. Our results showed that at 14 days after transplantation, the thickness of the regenerated epidermis was greater in the samples with MGCTs compared with micronized skin connective tissue (MG-skin).

In regards to the paracrine functions of MGCTs including vascularization, mesenchymal stem/progenitor cells in MGCTs must function in the manner mentioned above. Moreover, it is known that exogenous MSCs can promote vascularization at injury sites in various tissues (Wu et al., 2007). For

instance, bone marrow-derived MSCs (BMMSCs) have been shown to promote wound healing via direct differentiation (to an epidermal cell lineage) and the release of proangiogenic factors (Wu et al., 2007). In this study, blood vessel formation in the atelocollagen matrix was enhanced by co-transplantation with MGCTs. However, the obvious expression of porcine mRNA markers related to blood vessels (*cd31*, *vWF*) and epithelial cells (*cytokeratin*) was not observed clearly in MGCT samples, even though donor-derived mesenchymal cells likely survived until 2 weeks after transplantation. These phenomena suggest that the promotion of wound repair by MGCTs is due to the release of paracrine factors including proangiogenic factors, but not to the direct differentiation of MGCTs into endothelial or epithelial cells. Actually, we found the SDF-1/CXCR-4 signal pathway was significantly up-regulated in wound-area by MGCT transplantation. SDF-1/CXCR-4 pathway can facilitate the wound healing through augmenting BMMSC recruitment to the wound sites (Xu et al., 2013). In addition, our preliminary data using proteome profile array showed the increased expression levels of proangiogenic factors, such as Angiogenin, EGF, FGF, IGF, IP-10, KC, MMP-3, -9, SDF-1 and VEGF, in MGCTs at 7 days after transplantation (Supplemental Figure). As mentioned above, MGCTs contain not only stem/progenitor cells but also ECM components and various growth factors. Previous studies demonstrated that remodeling of the ECM components, such as Matrix Metalloproteinases (MMPs) and Tissue Inhibitor of Metalloproteinases (TIMPs), was more rapid and intense with gingival fibroblasts than dermal fibroblasts (Chaussain et al., 2002; Mah et al., 2014; Tarzemany et al., 2015). Furthermore, gingival fibroblasts express elevated levels of molecules involved in the regulation of

inflammation (Mah et al., 2014). Therefore, we can speculate that such components in gingival fibroblasts were contained in MGCTs and likely led to the enhanced wound healing without scar contraction observed in this study. Indeed, decreased scar contraction was clearly observed in samples with MGCTs, and the regeneration of skin appendages was detected in those samples at 3 weeks post-transplantation.

In conclusion, our results demonstrated that the micro-graft of MGCTs using the Rigenera® system can be effectively employed for skin regeneration without the need for complicated procedures. Our findings suggest that this strategy can be easily applied to the clinical setting, showing low morbidity and ready availability, and can contribute to keratinized gingival tissue reconstruction or augmentation as an alternative to FGG or CTG. Further investigations using more concrete animal models and clinical studies are needed to confirm our *in vivo* observations.

Acknowledgments

The authors wish to thank Mr. Tetsumaru Murata and Ms. Taki Yamada (TMSC Co., Ltd) for providing technical assistance with the Rigenera® system. The authors also thank Ms. Naoko Sakashita (Nagasaki University) for providing technical assistance with the experiments. All authors declare that there are no conflicts of interest.

References

Agarwal C, Tarun Kumar AB, Mehta DS. 2015. Comparative evaluation of free gingival graft and AlloDerm® in enhancing the width of attached gingival. Contemp Clin Dent 6:483–488.

Agata H, Asahina I, Watanabe N, Ishii Y, Kubo N, Ohshima S, Yamazaki M, Tojo A, Kagami H. 2010. Characteristic Change and Loss of In Vivo Osteogenic Abilities of Human Bone Marrow Stromal Cells During Passage. Tissue Eng Part A 16:663-673.

Basegmez C, Karabuda ZC, Demirel K, Yalcin S. 2013. The comparison of acellular dermal matrix allografts with free gingival grafts in the augmentation of peri-implant attached mucosa: a randomised controlled trial. Eur J Oral Implantol 6:145-152.

Basiouny HS,Salama NM, Maadawi ZM, Farag EA. 2011. Effect of Bone Marrow Derived Mesenchymal Stem Cells on Healing of Induced Full-Thickness Skin Wounds in Albino Rat. Int J Stem Cells. 6:12-25.

Boink MA, van den Broek LJ, Roffel S, Nazmi K, Bolscher JG, Gefen A, Veerman EC, Gibbs S. 2015. Different wound healing properties of dermis, adipose, and gingiva mesenchymal stromal cells. Wound Repair Regen 24:100-109.

Brito C, Tenenbaum HC, Wong BK, Schmitt C, Nogueira-Filho G. 2014. Is keratinized mucosa indispensable to maintain peri-implant health? A systematic review of the literature. J Biomed Mater Res B Appl Biomater 102:643-650.

Chaussain Miller C, Septier D, Bonnefoix M, Lecolle S, Lebreton-Decoster C, Coulomb B, Pellat B, Godeau G. 2002. Human dermal and gingival fibroblasts in a three-dimensional culture: a comparative study on matrix remodeling. Clin Oral Investig 6:39-50.

Fournier BP, Larjava H, Häkkinen L. 2013. Gingiva as a Source of Stem Cells with Therapeutic Potential. Stem Cells and Dev 22:3157-3177.

Giaccone M,Brunetti M,Camandona M, Trovato L, Graziano A. 2014. A New Medical Device, Based on Rigenera Protocol, in the Management of Complex Wounds. J Stem Cells Res, Rev & Rep 1:1013.

Herford AS, Akin L, Cicciu M, Maiorana C, Boyne PJ. 2010. Use of a porcine collagen matrix as an alternative to autogenous tissue for grafting oral soft tissue defects. J Oral Maxillofac Surg 68:1463-1470.

I T, Sumita Y, Minamizato T, Umebayashi M, Liu Y, Tran SD, Asahina I. 2014. Bone Marrow-derived Cell Therapy for Oral Mucosal Repair after Irradiation. J Dent Res 93:813-820.

Imaizumi F, Asahina I, Moriyama T, Ishii M, Omura K. 2004. Cultured Mucosal Cell Sheet with a Double Layer of Keratinocytes and Fibroblasts on a Collagen Membrane. Tissue Eng 10:657-664.

Kim BS, Kim YK, Yun PY, Yi YJ, Lee HJ, Kim SG, Son JS. 2009. Evaluation of peri-implant tissue response according to the presence of keratinized mucosa. Oral Surg Oral Med Oral Pathol Oral Radiol Endod 107:24–28.

Lin GH, Chan HL, Wang HL. 2013. The significance of keratinized mucosa on implant health: a systematic review. J Periodontol 84:1755-1767.

Mah W, Jiang G, Olver D, Cheung G, Kim B, Larjava H, Häkkinen L.2014. Human Gingival Fibroblasts Display a Non-Fibrotic Phenotype Distinct from Skin Fibroblasts in Three-Dimensional Cultures. PLoS One 9:e90715.

Marcarelli M, Trovato L, Novarese E, Riccio M, Graziano A. 2016. Rigenera protocol in the treatment of surgical wound dehiscence. Int Wound J. 2016 Apr 29 [Epub ahead of print].

Monti M, Graziano A, Rizzo S, Perotti C, Del Fante C, d'Aquino R, Redi C, Rodriguez Y Baena R. 2016. In Vitro and In Vivo Differentiation of Progenitor Stem Cells Obtained After Mechanical Digestion of Human Dental Pulp. 2016 Jun 9 [Epub ahead of print].

Schmitt CM, Tudor C, Kiener K, Wehrhan F, Schmitt J, Eitner S, Agaimy A, Schlegel KA. 2013. Vestibuloplasty: Porcine Collagen Matrix Versus Free Gingival Graft: A Clinical and Histologic Study. J Periodontol 84:914-923

Schmitt CM, Moest T, Lutz R, Wehrhan F, Neukam FW, Schlegel KA. 2015. Long-term outcomes after vestibuloplasty with a porcine collagen matrix (Mucograft®) versus the free gingival graft: a comparative prospective clinical trial. Clin Oral Implants Research 00:1-9.

Schrott AR, Jimenez M, Hwang JW, Fiorellini J, Weber HP. 2009. Five-year evaluation of the influence of keratinized mucosa on peri-implant soft-tissue health and stability around implants supporting full-arch mandibular fixed prostheses. Clin Oral Implants Res 20: 1170–1177.

Sumita Y, Liu Y, Khalili S, Maria OM, Xia D, Key S, Cotrim AP, Mezey E, Tran SD.2011. Bone marrow-derived cells rescue salivary gland function in mice with head and neck irradiation. Int J Biochem Cell Biol 43:80-87.

Svolacchia F, De Francesco F, Trovato L, Graziano A, Ferraro GA. 2016. An innovative regenerative treatment of scars with dermal micrografts. J Cosmet Dermatol 15:245-53.

Tarzemany R, Jiang G, Larjava H, Häkkinen L. 2015. Expression and function of connexin 43 in human gingival wound healing and fibroblasts. PLoS One 10:e0115524.

Thoma DS, Benić GI, Zwahlen M, Hämmerle CH, Jung RE. 2009. A systematic review assessing soft tissue augmentation techniques. Clin Oral Implants Res 4:146-165.

Trovato L, Monti M, Del Fante C, Cervio M, Lampinen M, Ambrosio L, Redi CA, Perotti C, Kankuri E, Ambrosio G, Rodriguez Y Baena R, Pirozzi G, Graziano A. 2015. A New Medical Device Rigeneracons Allows to Obtain Viable Micro-Grafts From Mechanical Disaggregation of Human Tissues. J Cell Physiol. 230:2299-2303.

van den Bogaerdt AJ, van der Veen VC, van Zuijlen PP, Reijnen L, Verkerk M, Bank RA, Middelkoop E, Ulrich MM. 2009. Collagen cross-linking by adipose-derived mesenchymal stromal cells and scar-derived mesenchymal cells: Are mesenchymal stromal cells involved in scar formation? Wound Repair Regen 17:548-58.

van den Broek LJ, Limandjaja GC, Niessen FB, Gibbs S. 2014. Human hypertrophic and keloid scar models: principles, limitations and future challenges from a tissue engineering perspective. Exp Dermatol 23:382-386.

Wu Y, Chen L, Scott PG, Tredget EE. 2007. Mesenchymal Stem Cells Enhance Wound Healing Through Differentiation and Angiogenesis. Stem Cells 25:2648-59.

Xia D, Sumita Y, Liu Y, Tai Y, Wang J, Uehara M, Agata H, Kagami H, Fan Z, Asahina I, Wang S, Tran SD. 2013. GDFs promote tenogenic characteristics on human periodontal ligament-derived cells in culture at late passages. Growth Factors 31:165-173.

Xu X, Zhu F, Zhang M, Zeng D, Luo D, Liu G, Cui W, Wang S, Guo W, Xing W, Liang H, Li L, Fu X, Jiang J, Huang H. 2013. Stromal cell-derived factor-1 enhances wound healing through recruiting bone marrow-derived mesenchymal stem cells to the wound area and promoting neovascularization. Cells Tissues Organs 197:103-113.

Yoo G, Lim JS. 2009. Tissue Engineering of Injectable Soft tissue Filler: Using Adipose Stem Cells and Micronized Acellular Dermal Matrix. J Korean Med Sci 24:104–109.

Zanzottera F, Lavezzari E, Trovato L, Icardi A, Graziano A. 2014. Adipose Derived Stem Cells and Growth Factors Applied on Hair Transplantation. Follow-Up of Clinical Outcome. SciRes. Scientific Reserch. 4:268-274.

Zhang Q, Su WR, Shi SH, Wilder-Smith P, Xiang AP, Wong A, Nguyen AL, Kwon CW, Le AD. 2010. Human Gingiva-Derived Mesenchymal Stem Cells Elicit Polarization of M2 Macrophages and Enhance Cutaneous Wound Healing. Stem Cells 28:1856–1868.

Zhang QZ, Nguyen AL, Yu WH, Le AD. 2012. Human Oral Mucosa and Gingiva:A Unique Reservoir for Mesenchymal Stem Cells. J Dent Res 91:1011–1018.

Figure legends

Figure 1. Procedures of micro-graft with MGCTs to the skin defect. **(A)** 2-cubic millimeters of gingival connective tissue was harvested from the porcine palatal gingiva (box area). **(B)** Rigenera machine® (left) and Rigeneracons® (right) (Human Brain Wave, Italy). **(C)** Outgrowth of fibroblastic cells from an adherent MGCT at 7 days of culture. These cells were positive (green) for anti-Vimentin cytostaining. **(D)** Gross appearance of atelocollagen-matrix with MGCTs before transplantation. **(E)** Round full-thickness excisional wound (5 mm in diameter). 4 tattoo marks were delineated at the place of 1 mm away from the wound margin. **(F)** Gross appearance after transplantation of samples.

Figure 2. Macroscopic findings after treatment. **(A)** Gross appearance of wounds in MG, AC and Control groups at 7, 14, 21 days post-transplantation (each group; n=5 at each time points). Yellow-dotted line: boundary of unhealed wound area. Red arrow head: portions of tattoo marks. **(B)** Changes of percentage of wound reduction (area of actual wound / area of original wound) at 7, 14, 21 days post-transplantation (each group; n=5 at each time points). **(C)** Changes of percentage of Scar-contraction area at 7, 14, 21 days post-transplantation (each group; n=5 at each time points).

Figure 3. Histological analysis of wound-areas at Day 14 post-transplantation (each group; n=5). **(A-H)** HE staining of wound-areas in MG **(A)**, AC **(C)**, Control **(E)** and MG-skin **(G)** samples (scale bar is 200 μm), and Masson's trichrome staining of wound-areas in MG **(B)**, AC **(D)**, Control **(F)** and MG-skin **(H)** samples

(scale bar is 500 μm). Red arrow head: re-epithelialized portions. Red asterisks: transplanted-matrix portions. **(I)** Epithelial thickness of wound-area in MG and MG-skin group. (3 sets of consecutive 3 sections/specimen for each group; n=3)

Figure 4. Histological analysis of wound-areas at Day 21 post-transplantation (each group; n=5). **(A)** HE staining of wound-areas in MG samples (scale bar is 200 μm) (left), and Cytokeratin immunohistochemical staining of box area is shown in higher magnification (scale bar is 200 μm) (right). Cytokeratin-positive skin appendages (arrow heads) are recognized. **(B)** HE staining of wound-areas in AC samples (scale bar is 400 μm) (left), and Cytokeratin immunohistochemical staining of box area is shown in higher magnification (scale bar is 200 μm) (right). The portion of incomplete epithelization in wound area is observed as Cytokeratin-negative. **(C)** HE staining of wound-areas in Control samples (scale bar is 500 μm).

Figure 5. Blood vessels formation in wound-area. **(A, B)** CD31 (green-fluorescent) and vWF (red-fluorescent) immunofluorescence staining in matrix adjacent to wound-area in MG **(A)** and AC **(B)** samples at Day 14 post-transplantation (scale bar is 100 μm). The box area in **(A)** is shown in higher magnification. Yellow dotted line: Boundary of the epithelium and dermis. Blue: DAPI. **(C)** Time course of Blood vessel formation. (5 randomly fields/section in 5 sections/specimen for each group; n=3 at each time points)

Figure 6. Detection of MGCT-derived cells and tissue regenerative factors in wound-area at 7 and 14 days post-transplantation. **(A)** PKH26 (red-fluorescent)-labeled cells were recognized in matrix of MG samples but not in that of AC samples at 7 days (scale bar is 50 μm) (each group; n=3). The box area just below the area that will be epithelized is shown in higher magnification. Yellow dotted line: Boundary of the epithelium and dermis. Blue: DAPI. **(B)** Expression of porcine-specific mRNAs (*vimentin*, *vWF*, *cd31*, *cytokeratin* and *β-actin*) in Control, Pig, MG and AC samples at 14 days (each group; n=3). Vimentin-gene expression is detected in MG samples as with Pig samples. **(C)** Expression levels of mouse-specific genes, related to the tissue regenerative/angiocrine factors in MG and AC samples at 7 days (each group; n=3).

Table 1: Sequence of porcine specific primer pairs for RT-PCR

gene	*sense*	*anti-sense*
vimentin	5'-GGAACAGCACGTCCAAATCG-3'	5'-CGCATCCACTTCACAGGTGA-3'
vWF	5'-GCAGATAGACTGGGATGGCC-3'	5'-GGTTGCCGTTGTAATTCCCG-3'
cd31	5'-CCAGCCGCATTTCCAAAGTC-3'	5'-GCTCTGAGGCTACCTTGGTG-3'
cytokeratin	5'-AAGAGCACATGGCAGGACTT-3'	5'-CTTGGAGGTGGCTTCAGTTC-3'
β-actin	5'-GACCGACTACCTCATGAAG-3'	5'-CCGTGATCTCCTTCTGCAT-3'

,

Table 2

Table 2: Sequence of mouse specific primer pairs for quantitative-PCR

gene	*sense*	*anti-sense*
Sdf-1	5'- CCAACGTCAAGCATCTGAAA-3'	5'- TAATTTCGGGTCAATGCACA-3'
cxcr-4	5'-TGGAACCGATCAGTGTGAGT-3'	5'-GATGGTGGGCAGGAAGATCC-3'
vegf-a	5'-CCTCCGAAACCATGAACTTT-3'	5'-TCATGGGACTTCTGCTCTCC-3'
Vegf-b	5'-CTCATGATCCAGTACCCGAGC-3'	5'-GCTTCACAGCACTCTCCTTT-3'
flt-1	5'-CTCACTTGCACCGTGTATGG-3'	5'- TGCTGGGATCCAGGATAAAG-3'
flk-1	5'-GCTTGCCTTATGATGCCAGC-3'	5'-TCCAAAAGCGTCTGCCTCAA-3'
gapdh	5'-GGATGCAGGGATGATGTTC-3'	5'-TGCACCACCAACTGCTTAG-3'

Figure 1

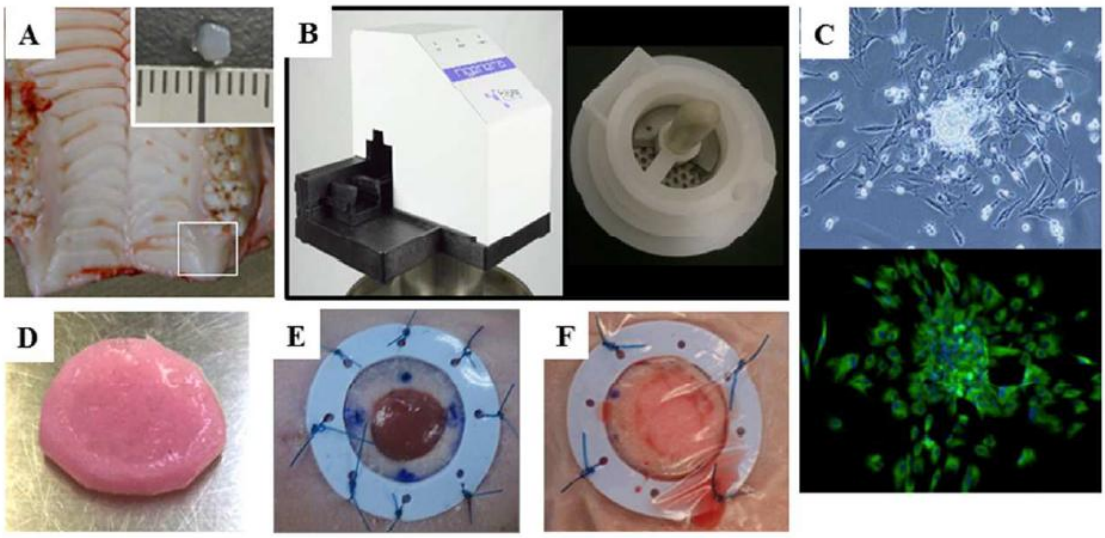

Figure 2

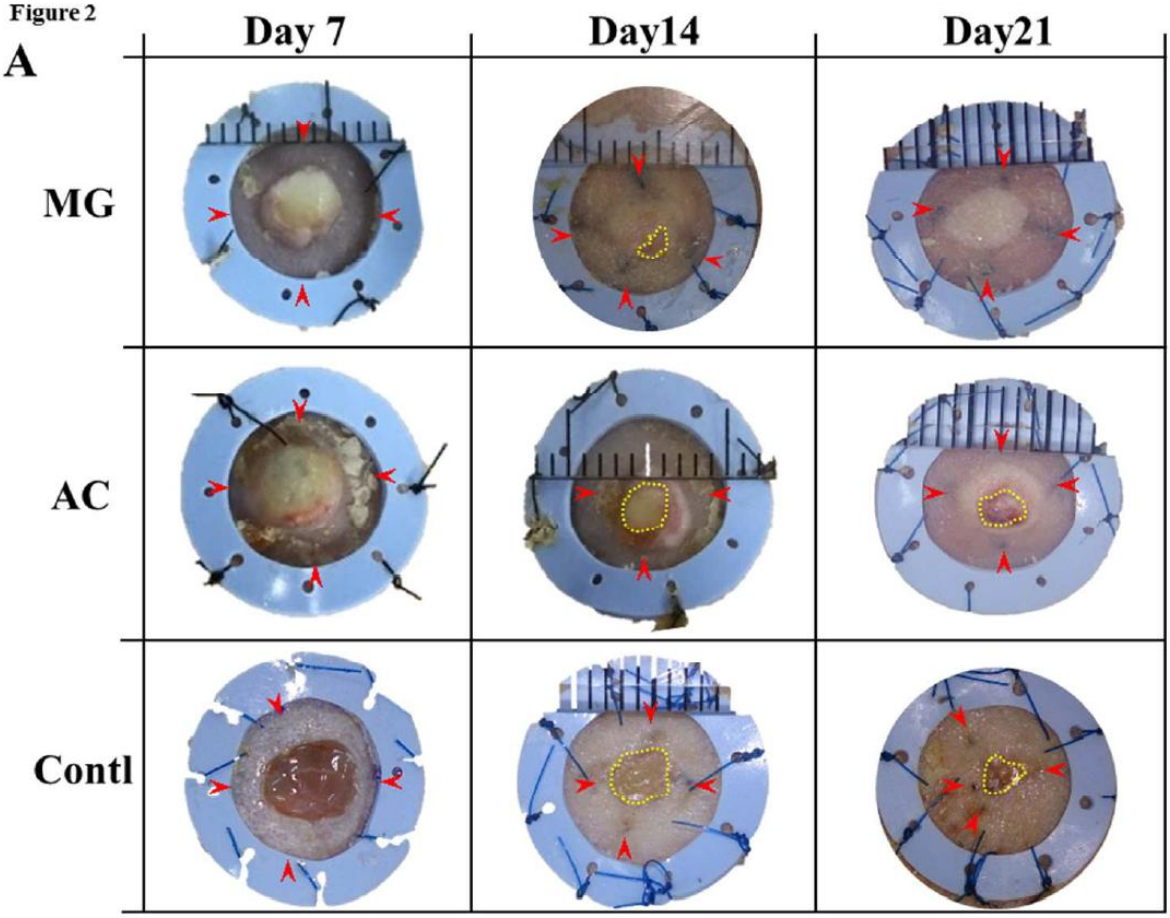

Figure 2

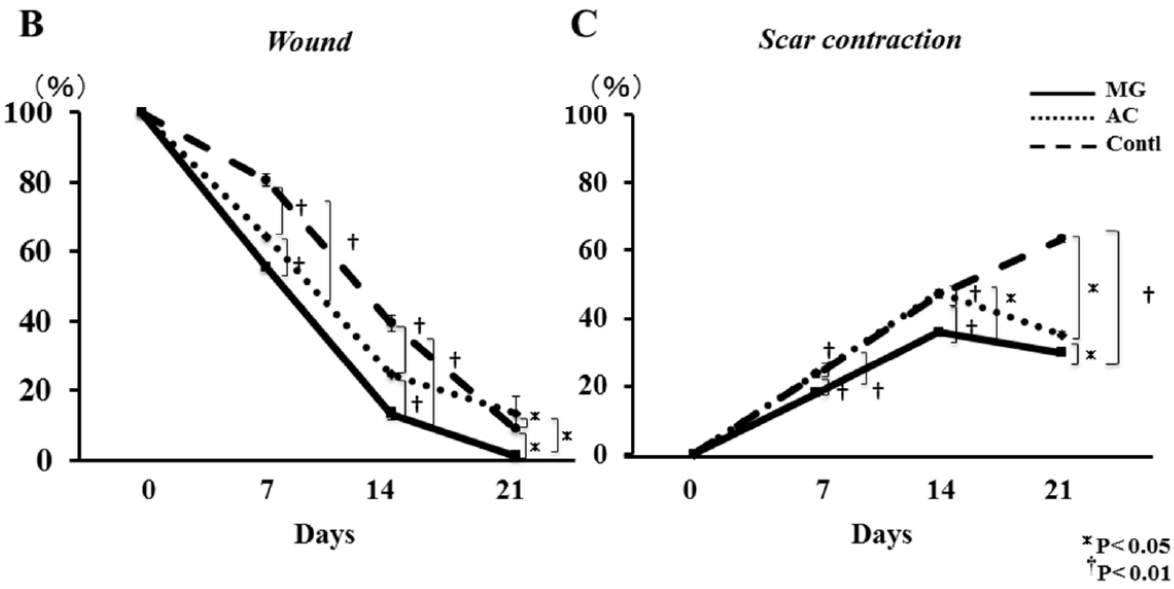

Figure 3

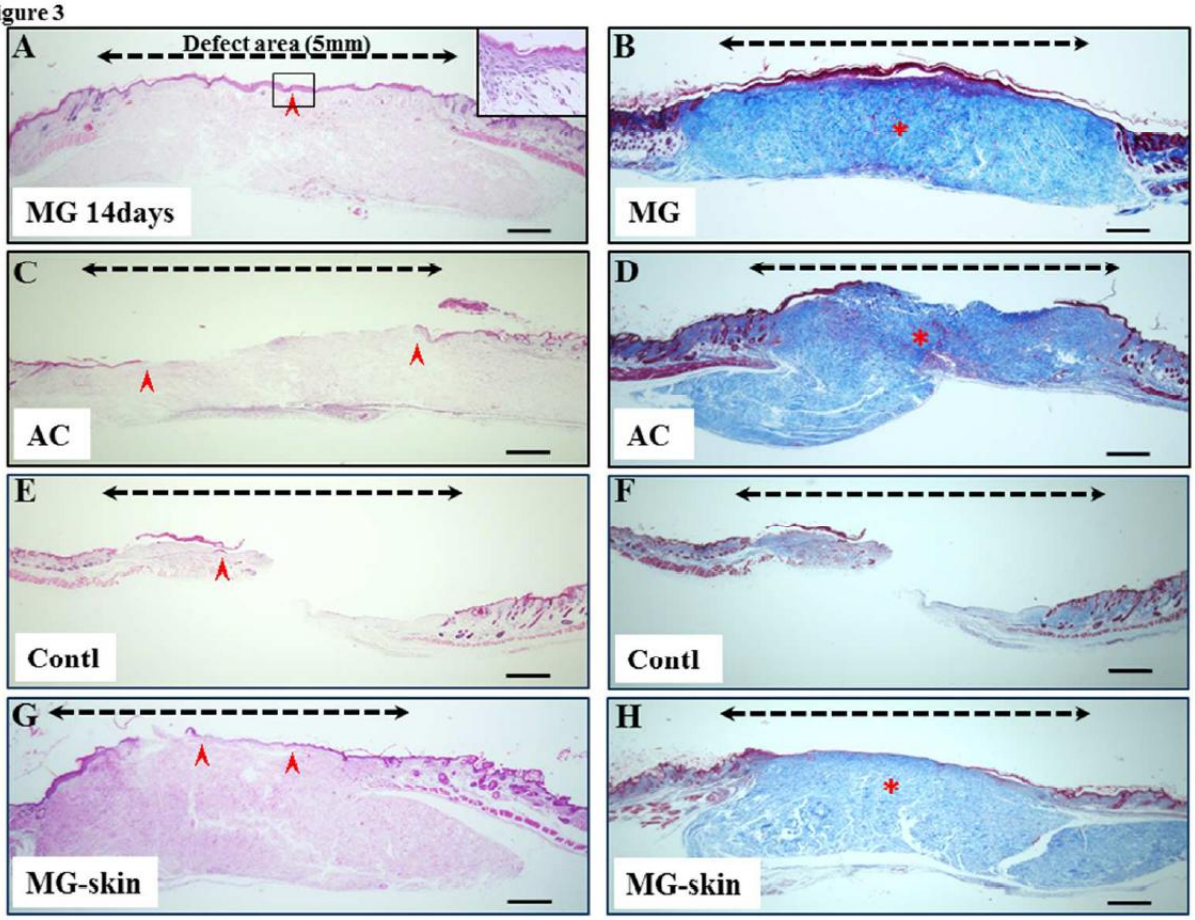

Figure 3

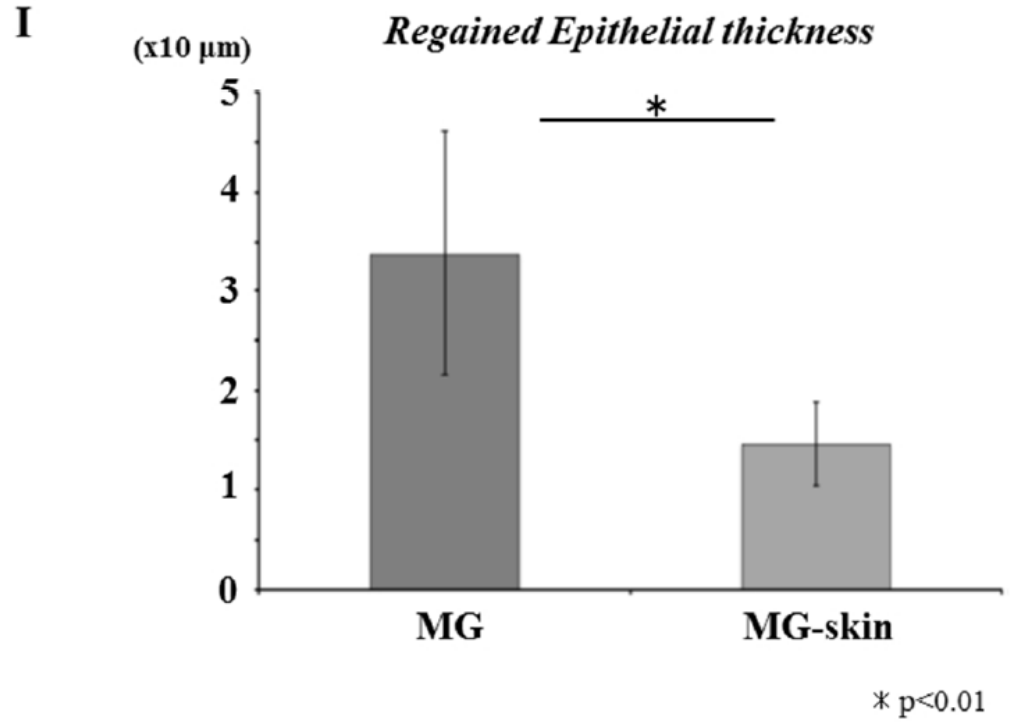

Figure 4

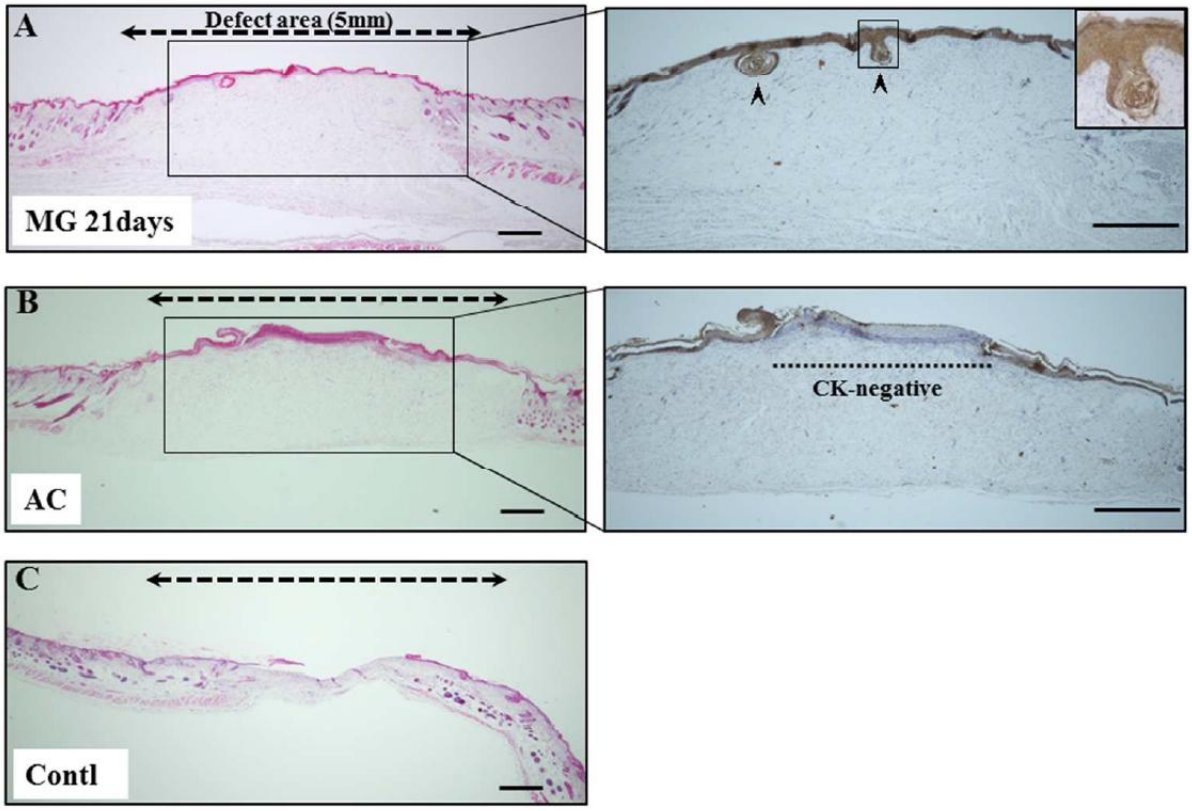

Figure 5

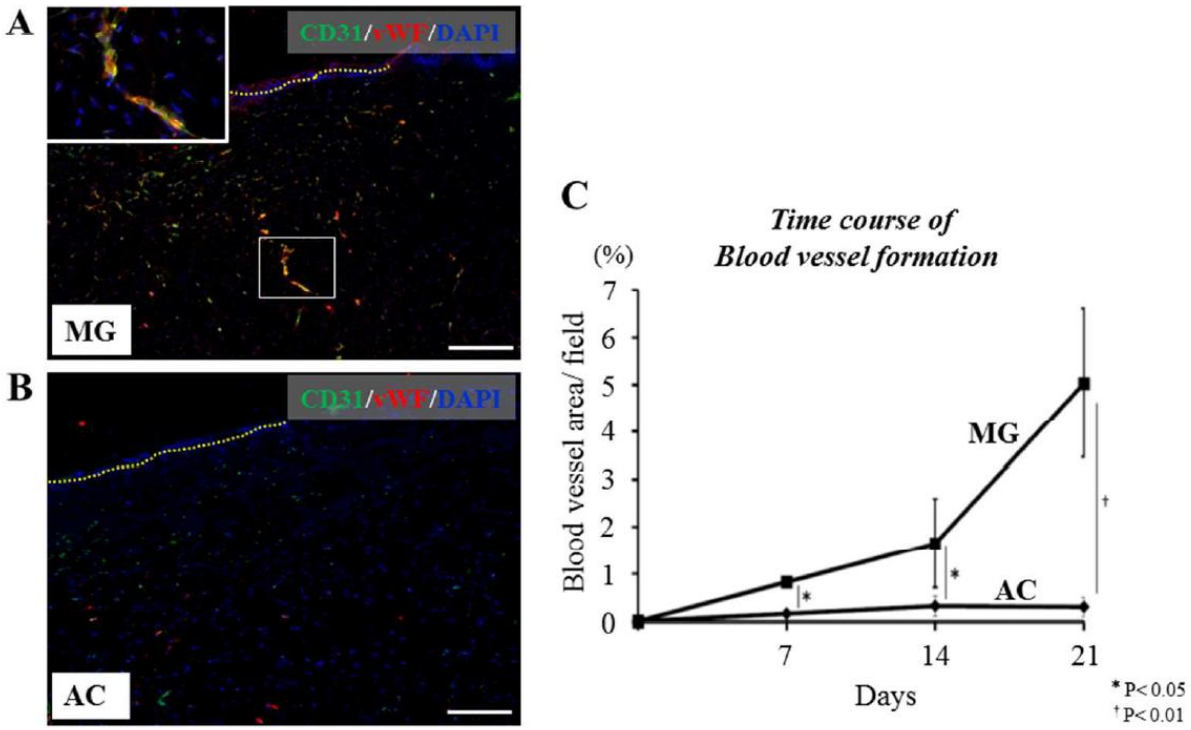

Figure 6

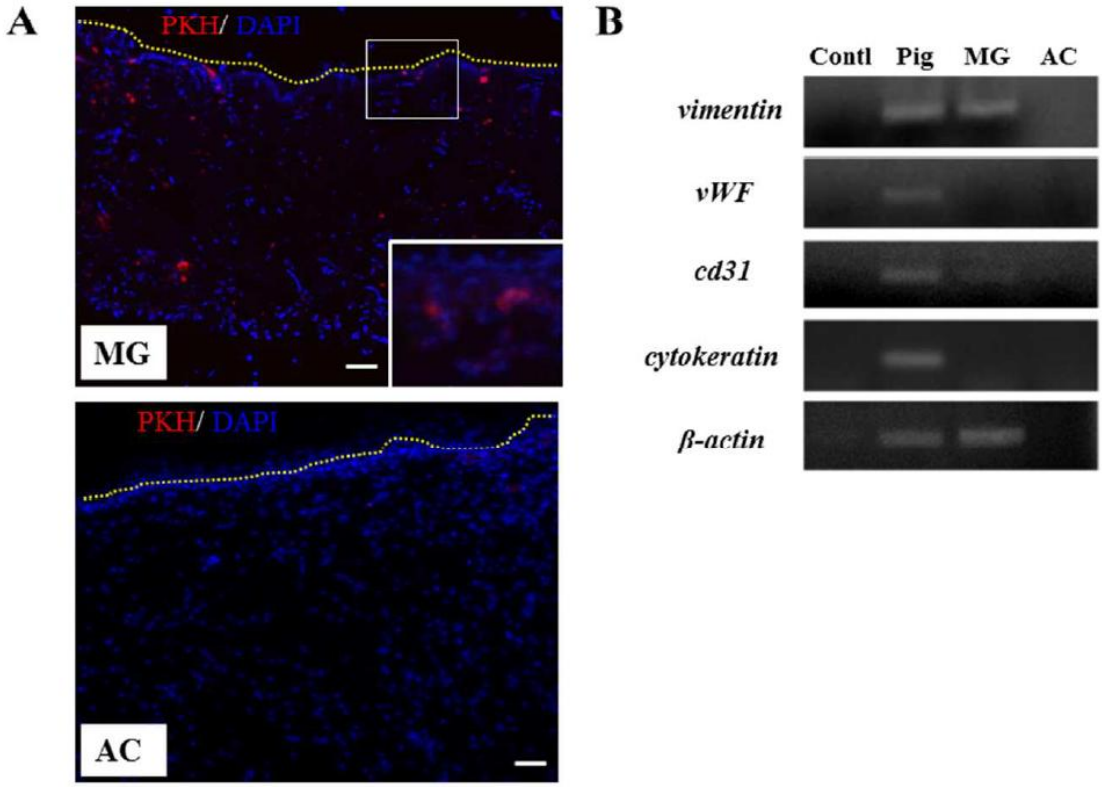

Figure 6